NeuroImage 54 (2011) 191–202

Contents lists available at ScienceDirect

NeuroImage

journal homepage: www.elsevier.com/locate/ynimg

Hemisphere- and gender-related differences in small-world brain networks: A resting-state functional MRI study

Lixia Tian [a], Jinhui Wang [b], Chaogan Yan [b], Yong He [b,*]

[a] Department of Biomedical Engineering, School of Computer Science and Information Technology, Beijing Jiaotong University, Beijing, 100044, China
[b] State Key Laboratory of Cognitive Neuroscience and Learning, Beijing Normal University, Beijing, 100875, China

ARTICLE INFO

Article history:
Received 2 June 2010
Revised 25 July 2010
Accepted 27 July 2010
Available online 3 August 2010

Keywords:
Resting-state fMRI
Functional connectivity
Efficiency
Asymmetry
Graph theory

ABSTRACT

We employed resting-state functional MRI (R-fMRI) to investigate hemisphere- and gender-related differences in the topological organization of human brain functional networks. Brain networks were first constructed by measuring inter-regional temporal correlations of R-fMRI data within each hemisphere in 86 young, healthy, right-handed adults (38 males and 48 females) followed by a graph-theory analysis. The hemispheric networks exhibit small-world attributes (high clustering and short paths) that are compatible with previous results in the whole-brain functional networks. Furthermore, we found that compared with females, males have a higher normalized clustering coefficient in the right hemispheric network but a lower clustering coefficient in the left hemispheric network, suggesting a gender–hemisphere interaction. Moreover, we observed significant hemisphere-related differences in the regional nodal characteristics in various brain regions, such as the frontal and occipital regions (leftward asymmetry) and the temporal regions (rightward asymmetry), findings that are consistent with previous studies of brain structural and functional asymmetries. Together, our results suggest that the topological organization of human brain functional networks is associated with gender and hemispheres, and they provide insights into the understanding of functional substrates underlying individual differences in behaviors and cognition.

Introduction

The human brain is asymmetric in terms of structure and function (for a review, see Toga and Thompson, 2003). The structural asymmetries of the brain have been well-documented. For example, besides the well-known frontal (right>left) and occipital (left>right) petalias (Watkins et al., 2001; Lancaster et al., 2003; Narr et al., 2007), leftward volume asymmetries have been consistently observed in brain regions specialized for language (Good et al., 2001; Pujol et al., 2002). Functional asymmetries of the brain have been repeatedly reported to exist in a variety of functions such as language, motor, and visuospatial processing (for a review, see Toga and Thompson, 2003). It has been suggested that alterations of brain asymmetries are associated with behavior changes in normal aging (Kovalev et al., 2003; Bergerbest et al., 2009) and in various neuropsychiatric and neurological diseases such as schizophrenia (Bilder et al., 1999; Niznikiewicz et al., 2000; Sommer et al., 2001; Narr et al., 2001; Bleich-Cohen et al., 2009), stroke (Liepert et al., 2000; Tecchio et al., 2006a,b, 2007) and dyslexia (Leonard et al., 2001; Heim et al., 2003; Leonard and Eckert, 2008).

Some aspects of brain asymmetries also interact with gender. Research in gender-related differences in brain asymmetries began several decades ago. Kulynych et al. (1994) reported that males have a greater structural asymmetry of the plenum temporal than females. Hiscock et al. (1994, 1995) demonstrated that the male brain is more functionally lateralized or asymmetric in visual and auditory areas than the female brain. Shaywitz et al. (1995) observed that phonological processing aroused activation in the left inferior frontal gyrus (IFG) in males, but the bilateral IFG was activated in females. Closely related to these results, gender differences have also been demonstrated in behaviors. Statistically, males perform better in right-lateralized visuospatial perception processing, whereas females have advantages in the left-lateralized language processing (Hamilton, 2008). The gender differences in brain asymmetries have been suggested as the underlying origin of gender differences in lateralized behaviors (Kimura, 1999).

Despite the advances in brain asymmetry research, however, little is known about whether there are differences in the topological organization of brain networks between the hemispheres and whether those differences are related to gender. Graph theoretical analysis provides a powerful tool to characterize the topological organization of complex networks, and it has recently been applied to the study of human brain networks in health and disease (for reviews, see Bullmore and Sporns, 2009; Bassett and Bullmore, 2009; He et al., 2009a; He and Evans, 2010). Using graph theoretical approaches,

* Corresponding author.
E-mail address: yong.he@bnu.edu.cn (Y. He).

1053-8119/$ – see front matter © 2010 Elsevier Inc. All rights reserved.
doi:10.1016/j.neuroimage.2010.07.066

researchers have demonstrated that the structural and functional networks of the human brain constructed by a variety of neuroimaging modalities (e.g., structural MRI, functional MRI, and diffusion MRI) have non-trivial topological attributes such as the small-world property (high clustering and short path lengths linking different nodes [Watts and Strogatz, 1998]) (Salvador et al., 2005; Achard et al., 2006; Hagmann et al., 2007; He et al., 2007), high network efficiency at a low wiring cost (Achard et al., 2006; He et al., 2009b), and highly connected network hubs (Achard et al., 2006; He et al., 2007; Bassett et al., 2008; Hagmann et al., 2008; Gong et al., 2009a; He et al., 2009c). It is noteworthy that almost all of these previous studies of brain networks focused on *whole-brain* level graphic analyses. To date only one study examined hemisphere-related differences in the topological organization of structural brain networks in right-handed subjects using diffusion-weighted MRI tractography; it was found that the right hemisphere is more efficient and interconnected than the left hemisphere (Iturria-Medina et al., in press). However, no study has reported hemisphere-related differences in the topological organization of brain functional networks. Moreover, very little is known about whether the topological organization is associated with gender.

Here, we utilized resting-state functional MRI (R-fMRI) to investigate hemisphere- and gender-related differences in the organizational patterns of functional networks in the human brain. R-fMRI has recently attracted considerable attention as a novel, non-invasive way to measure intrinsic or spontaneous activity in the brain (Biswal et al., 1995; for reviews, see Fox and Raichle, 2007; Zhang and Raichle, 2010). Advances in graph theoretical analysis of R-fMRI data have allowed us to map the topological organization of brain functional networks under normal and pathological conditions (for reviews, see Bullmore and Sporns, 2009; He et al., 2009a; Bassett and Bullmore, 2009; He and Evans, 2010; Wang et al., 2010). In this study, we sought to determine whether there are small-world attributes and high network efficiency within each hemisphere and whether these topological properties show hemisphere- or gender-related differences. To address these issues, we acquired R-fMRI data of 86 young, healthy, right-handed adults, and parcellated the brain into 90 cortical and subcortical regions according to a prior brain atlas (Tzourio-Mazoyer et al., 2002). Then we constructed brain functional networks by thresholding temporal correlations of spontaneous activity between any pairs of brain areas within each hemisphere and calculated the global and regional nodal parameters, as well as the asymmetries of these parameters. Finally, hemisphere- and gender-related differences in these network parameters were statistically evaluated.

Materials and methods

Subjects

Data were selected from a large sample resting-state fMRI dataset of our group, which has been publicly released in the "1000 Functional Connectomes" Project (http://www.nitrc.org/projects/fcon_1000/) (Biswal et al., 2010). We selected 86 young healthy volunteers (48 females: 20.8 ± 1.6 years old, range 18–25; and 38 males: 20.7 ± 1.7 years old, range 17–25) with head motion less than 2.0 mm displacement in any of the x, y, or z directions or 2.0° of any angular motion throughout the resting-state scan. All are right-handed and had no history of neurological and psychiatric disorders. Written informed consent was obtained from each participant, and the study was approved by the Institutional Review Board of Beijing Normal University Imaging Center for Brain Research. During the resting state, the subjects were instructed to keep still with their eyes closed but not fall asleep, remain as motionless as possible, and to think of nothing in particular. All the subjects had not fallen asleep according to a simple questionnaire after the scan.

Imaging acquisitions and data preprocessing

Resting data were obtained using a 3.0 T Siemens scanner at the Imaging Center for Brain Research, Beijing Normal University. A total of 240 volumes of EPI images were obtained axially (repetition time, 2000 ms; echo time, 30 ms; slices, 33; thickness, 3 mm; gap, 0.6 mm; field of view, 200×200 mm^2; resolution, 64×64; flip angle, 90°). Other images not used in the present study will not be described here.

Prior to preprocessing, the first 10 volumes were discarded to allow for scanner stabilization and the subjects' adaptation to the environment. R-fMRI data preprocessing was then conducted by SPM5 (http://www.fil.ion.ucl.ac.uk/spm/) and Data Processing Assistant for Resting-State fMRI (DPARSF) (Yan and Zang, 2010). Briefly, the remaining functional scans were first corrected for within-scan acquisition time differences between slices, and then realigned to the first volume to correct for inter-scan head motions. This realigning step provided a record of head motions within each fMRI run. Subsequently, the functional scans were spatially normalized to a standard template (Montreal Neurological Institute) and resampled to $3 \times 3 \times 3$ mm^3. The waveform of each voxel was finally passed through a band-pass filter (0.01–0.1 Hz) to reduce low-frequency drift and high-frequency physiological noise.

Construction of brain functional networks

To construct brain functional networks in this study, we first employed an automated anatomical labeling (AAL) atlas (Tzourio-Mazoyer et al., 2002) to parcellate the brain into 90 regions of interest (ROIs) (45 in each hemisphere). The names of the ROIs and their corresponding abbreviations are listed in Table 1. The time series was acquired on each ROI by averaging the signals of all voxels within that region and then linearly regressing out the influences of head motion and global signals. By calculating the Pearson correlation coefficient in the residual time courses between each pair of ROIs within the same

Table 1
The names and the corresponding abbreviations of the regions of interest (ROIs).

Region	Abbreviation	Region	Abbreviation
Precentral gyrus	PreCG	Lingual gyrus	LING
Superior frontal gyrus (dorsal)	SFGdor	Superior occipital gyrus	SOG
Orbitofrontal cortex (superior)	ORBsup	Middle occipital gyrus	MOG
Superior frontal gyrus (medial)	SFGmed	Inferior occipital gyrus	IOG
Orbitofrontal cortex (medial)	ORBmed	Fusiform gyrus	FFG
Middle frontal gyrus	MFG	Postcentral gyrus	PoCG
Orbitofrontal cortex (middle)	ORBmid	Superior parietal gyrus	SPG
Inferior frontal gyrus (opercula)	IFGoperc	Inferior parietal lobule	IPL
Inferior frontal gyrus (triangular)	IFGtriang	Supramarginal gyrus	SMG
Orbitofrontal cortex (inferior)	ORBinf	Angular gyrus	ANG
Rolandic operculum	ROL	Precuneus	PCUN
Supplementary motor area	SMA	Paracentral lobule	PCL
Olfactory	OLF	Caudate	CAU
Rectus gyrus	REC	Putamen	PUT
Insula	INS	Pallidum	PAL
Anterior cingulate gyrus	ACG	Thalamus	THA
Middle cingulate gyrus	MCG	Heschl gyrus	HES
Posterior cingulate gyrus	PCG	Superior temporal gyrus	STG
Hippocampus	HIP	Temporal pole (superior)	TPOsup
Parahippocampal gyrus	PHG	Middle temporal gyrus	MTG
Amygdala	AMYG	Temporal pole (middle)	TPOmid
Calcarine cortex	CAL	Inferior temporal gyrus	ITG
Cuneus	CUN		

hemisphere, two 45×45 correlation matrices were obtained for each subject, one for the left hemisphere and the other for the right hemisphere. Correlation coefficients represent the functional connectivity strength between the ROIs within the same hemisphere. Finally, each correlation matrix was thresholded into a binarized matrix with a fixed sparsity value (defined as the total number of edges in a network divided by the maximum possible number of edges). Setting a sparsity-specific threshold ensured that the networks of both hemispheres had the same number of edges or wiring cost. Specifically, we thresholded each correlation matrix repeatedly over a wide range of sparsity ($10\% \le s \le 46\%$) at the intervals of 0.01. This range of sparsity was chosen to allow prominent small-world properties in brain networks to be observed (Watts and Strogatz, 1998) (for details, see the Results section). Through this thresholding, unweighted graphs were obtained with the nodes representing brain regions and the edges representing functional relationships between brain regions. Further network analysis was based on the two sets of 45×45 binarized matrices for each subject.

Network analysis

Global network parameters

Six network metrics, including four small-world parameters (clustering coefficient, C_p, characteristic path length, L_p, normalized clustering coefficient, γ, and normalized shortest path length, λ) and two efficiency parameters (global efficiency, E_{glob}, and local efficiency, E_{loc}), were adopted to characterize the global topological organization of brain networks. These six parameters were referred to as global network parameters. For a given graph G with N nodes, the clustering coefficient C_p is defined as (Watts and Strogatz, 1998):

$$C_p = \frac{1}{N}\sum_{i\in G}\frac{E_i}{D_{nod}(i)(D_{nod}(i)-1)/2} \tag{1}$$

where $D_{nod}(i)$ is the degree (defined as the number of edges connected to the node) of node i, and E_i is the number of edges in G_i, the subgraph consisting of the neighbors of node i. The characteristic path length L_p is defined as (Newman, 2003):

$$L_p = \frac{1}{\frac{1}{N(N-1)}\left(\sum_{j\neq i\in G}\frac{1}{L_{ij}}\right)} \tag{2}$$

where L_{ij} is the shortest path length between nodes i and j. The global efficiency E_{glob} is defined as (Latora and Marchiori, 2001):

$$E_{glob} = \frac{1}{N(N-1)}\sum_{j\neq i\in G}\frac{1}{L_{ij}}. \tag{3}$$

The local efficiency of G is measured as (Latora and Marchiori, 2001):

$$E_{loc} = \frac{1}{N}\sum_{i\in G}E_{glob}(i) \tag{4}$$

where $E_{glob}(i)$ is the global efficiency of G_i. Of the four parameters, C_p and E_{loc} measure the local cliquishness of a network, and L_p and E_{glob} measure the overall routing efficiency of a network.

To examine the small-world properties, the normalized clustering coefficient $\gamma = C_p^{real}/C_p^{rand}$ and the normalized characteristic path length $\lambda = L_p^{real}/L_p^{rand}$ were computed (Watts and Strogatz, 1998). C_p^{real} and L_p^{real} are the clustering coefficient and the characteristic path length of real networks, and C_p^{rand} and L_p^{rand} represent the means of corresponding indices derived from 100 matched random networks that preserve the same number of nodes, edges, and degree distribution as the real networks (Maslov and Sneppen, 2002; Milo et al., 2002). Typically, a small-world network should meet the following criteria: $\gamma > 1$ and $\lambda \approx 1$ (Watts and Strogatz, 1998), or $\sigma = \gamma/\lambda > 1$ (Humphries et al., 2006).

Regional nodal parameters

To examine the regional characteristics of brain functional networks we considered three nodal metrics: the nodal degree

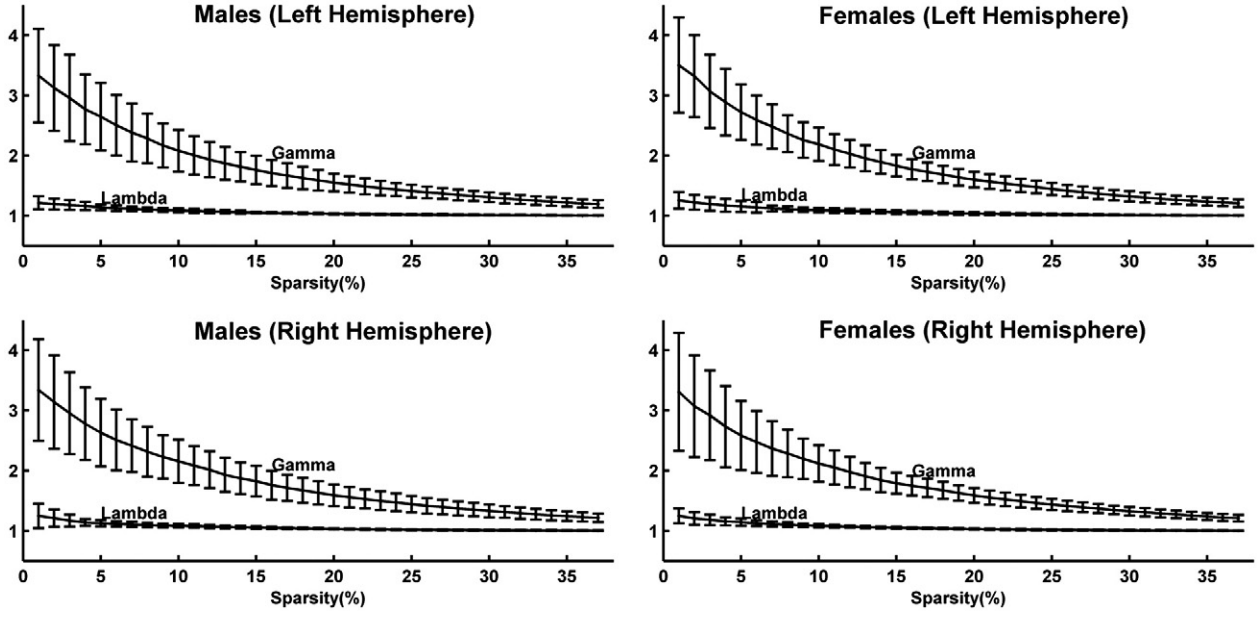

Fig. 1. Small-world properties of the hemispheric functional networks. The graphs show the changes in the γ and λ as a function of sparsity thresholds. The γ and λ were evaluated on the subjects' hemispheric networks and then averaged over the networks of the same subgroup: female left hemispheric networks; female right hemispheric networks; male left hemispheric networks; and male right hemispheric networks. At a wide range of sparsity, all the networks have an average γ of greater than 1 and an average λ of nearly 1, which implies prominent small-world properties.

(D_{nod}), the nodal efficiency (E_{nod}), and the nodal betweenness centrality (N_{bc}). The nodal degree of a node i is defined as:

$$D_{nod}(i) = \sum_{j \neq i \in G} e_{ij} \tag{5}$$

where e_{ij} is the (i,j)th element in the formerly obtained binarized correlation matrix. The nodal efficiency of a node i is defined as (Achard and Bullmore, 2007):

$$E_{nod}(i) = \frac{1}{N-1} \sum_{j \neq i \in G} \frac{1}{L_{ij}}. \tag{6}$$

The betweenness centrality of a node i is defined as (Freeman, 1977):

$$N_{bc}(i) = \sum_{j \neq i \neq k \in G} \frac{\delta_{jk}(i)}{\delta_{jk}} \tag{7}$$

where δ_{jk} is the number of shortest paths from node j to node k, and $\delta_{jk}(i)$ is the number of shortest paths from node j to node k that pass through node i within graph G. $N_{bc}(i)$ measures the influence of node i over information flow between other nodes in the whole network.

As for each network, we computed six global network parameters and three regional nodal parameters. To investigate the hemisphere-

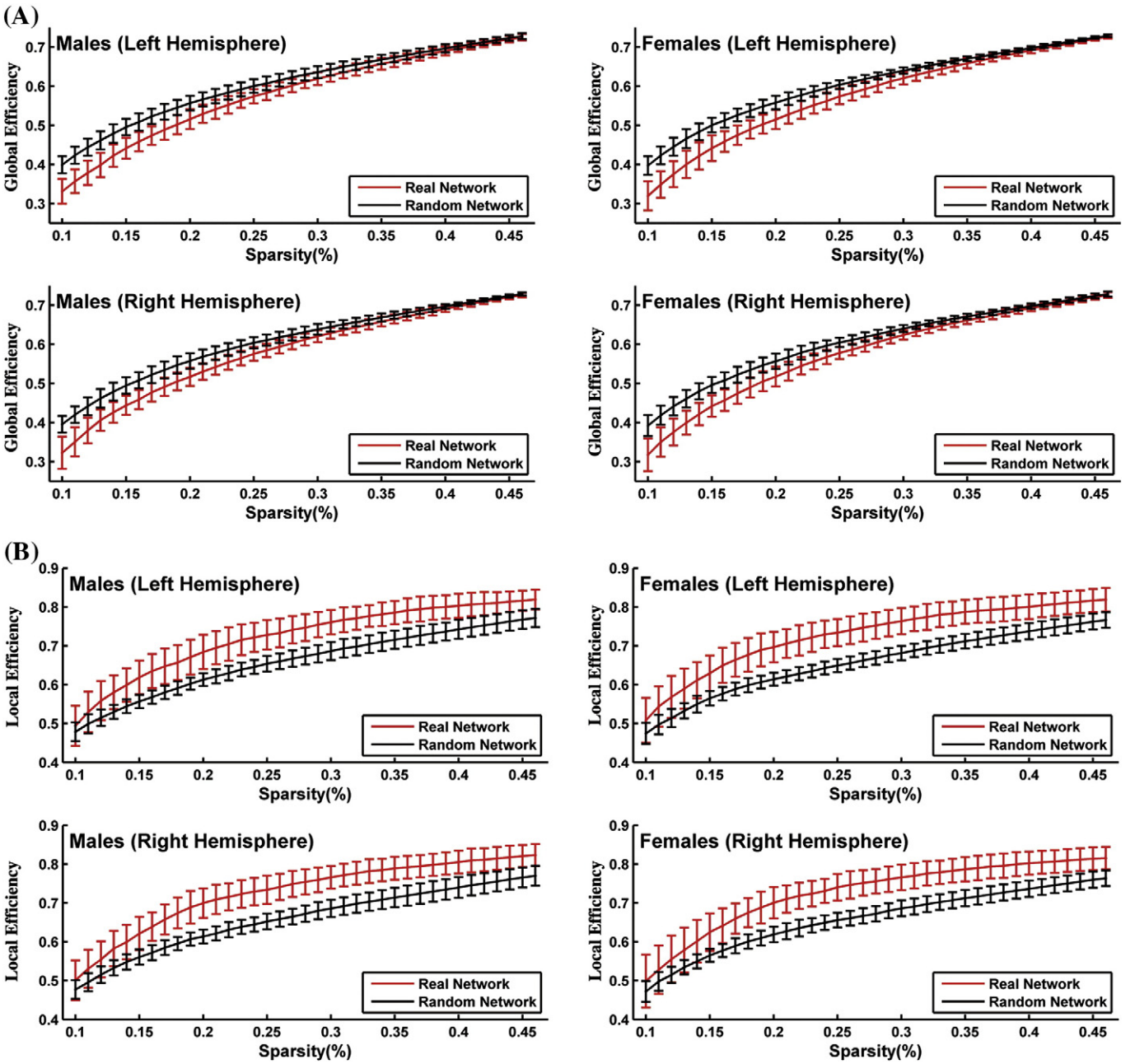

Fig. 2. The global efficiency (E_{glob}) (A) and local efficiency (E_{loc}) (B) of the hemispheric functional networks. The graphs show the changes in the E_{glob} and E_{loc} as a function of sparsity thresholds. The E_{glob} and E_{loc} were evaluated on the subjects' hemispheric networks and then averaged over the networks of the same subgroup. At a wide range of sparsity, all the networks have average E_{glob} comparable to that of the matched random networks and average E_{loc} larger than that of the matched random networks.

Table 2
Hemisphere and gender effects on global network parameters revealed by two-way repeated-measures ANOVA.

		C_p	L_p	γ	λ	E_{loc}	E_{glob}
Hemisphere effect	F-value	1.21	0.30	0.06	1.44	0.87	1.06
	P-value	0.27	0.58	0.81	0.23	0.35	0.31
Gender effect	F-value	0.13	0.03	0.26	0.63	0.23	0.03
	P-value	0.72	0.87	0.61	0.43	0.63	0.86
Interaction	F-value	2.04	0.05	**4.43**	1.00	1.89	0.07
	P-value	0.16	0.83	**0.04**	0.32	0.17	0.79

C_p, L_p, γ, λ, E_{loc} and E_{glob} denote the clustering coefficient, characteristic path length, normalized clustering coefficient, normalized shortest path length, local efficiency and global efficiency, respectively. Significant effects ($P<0.05$) are indicated by bold text.

and gender-related differences in these networks, we computed the integrated global network parameters as the summations:

$$X_{glob} = \sum_{k=10}^{46} X(k\Delta s)\,\Delta s \tag{8}$$

where Δs is the sparsity interval of 0.01; $X(k\Delta s)$ is a global network parameter (C_p, L_p, γ, λ, E_{loc} or E_{glob}) at a sparsity of $k\Delta s$. Similarly, the integrated regional nodal parameters of node i were calculated as the summations:

$$X_{nod}(i) = \sum_{k=10}^{46} X(i, k\Delta s)\Delta s \tag{9}$$

where $X(i,k\Delta s)$ is a nodal parameter (D_{nod}, E_{nod}, or N_{bc}) of the node i at a sparsity of $k\Delta s$. These integrated metrics were used to further identify network hubs and compute the hemisphere- and gender-related differences in the topological organization of the networks.

Hub identification

The nodes with the largest D_{nod}, E_{nod}, or N_{bc} values were considered hubs in the network. In this study, the hubs were identified based on four separate subgroups of networks: female left hemispheric networks; female right hemispheric networks; male left hemispheric networks; male right hemispheric networks. For each node we first calculated its normalized nodal parameters as follows:

$$X_{norm}(i) = \frac{\sum_{k=1}^{M} X_{nod}(i,k)/M}{\sum_{j=1}^{N}\sum_{k=1}^{M} X_{nod}(j,k)/(N\times M)} \tag{10}$$

where $X_{nod}(i,k)$ is an integrated nodal parameter (D_{nod},E_{nod}, or N_{bc}) of node i in the network of subject k, M is the number of networks in the subgroup and N is the number of nodes (here $N=45$). Node i was identified as the hub of the network if any of its three nodal parameters, $X_{norm}(i)$, was at least one standard deviation (SD) greater than the average of the parameter over the network (i.e., $X_{norm}(i) > mean + SD$).

Asymmetry score

The asymmetry of all network parameters was evaluated by the following asymmetry score:

$$A = 100 \times \frac{X(R) - X(L)}{0.5 \times (X(R) + X(L))} \tag{11}$$

where $X(R)$ and $X(L)$ are the parameters of the right and left hemispheres, respectively. Positive asymmetry scores indicated rightward asymmetry and vice versa.

Statistical analysis

Global network parameters

To determine whether there were significant differences in any of the six global network parameters, a two-way repeated-measures analysis of variance (ANOVA) was performed with gender as a between-subject factor and hemisphere (left and right) as a repeated-measures factor. If any main effect survived a threshold of $P<0.05$, a further t-test (paired t-test for the hemisphere effect and two-sample t-test for the gender effect) was performed. A two-tailed one-sample t-test was performed to determine whether the asymmetry scores of each of the six global network parameters within each gender was significantly different from zero. The asymmetry score of each global parameter was finally subjected to a two-tailed two-sample t-test to assess the between-gender differences. $P<0.05$ was considered to be significantly different.

Regional nodal parameters

The statistical analysis methods for the regional nodal parameters were similar to those for global network parameters. In brief, a two-way repeated-measures ANOVA was performed to determine the significant differences in the three regional nodal parameters and further t-tests were performed to determine the direction of these differences. T-tests were also performed for each region to evaluate the significance of the within- and between-gender differences in the asymmetry scores of the three regional nodal parameters. The threshold for all tests was $P<0.05$ (Bonferroni corrected).

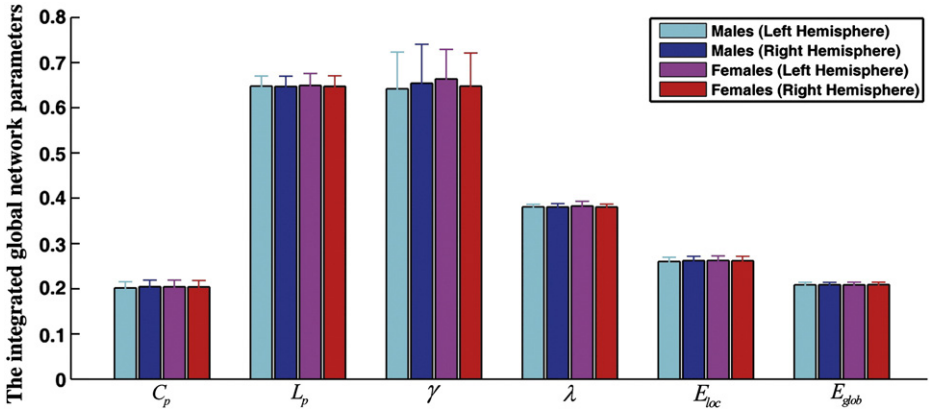

Fig. 3. The integrated global network parameters. C_p, L_p, γ, λ, E_{loc} and E_{glob} denote the clustering coefficient, characteristic path length, normalized clustering coefficient, normalized shortest path length, local efficiency and global efficiency, respectively. Note that the normalized clustering coefficient (γ) was greater in the right hemispheric networks of males, but greater in the left hemispheric networks of females (significant interaction: $P<0.05$).

Table 3
The asymmetry scores of the global network parameters.

		C_p	L_p	γ	λ	E_{loc}	E_{glob}
Females	T-score	−0.22	−0.53	−1.67	−1.48	−0.28	0.95
	P-value	0.82	0.60	0.10	0.14	0.78	0.35
Males	T-score	1.78	−0.26	1.44	−0.19	1.93	0.55
	P-value	0.08	0.80	0.16	0.85	0.06	0.58
Females–males	T-score	−1.38	−0.19	**−2.14**	−0.97	−1.36	0.27
	P-value	0.17	0.85	**0.04**	0.34	0.18	0.79

Females and Males indicate the significance of the asymmetry scores, and Females−Males indicates the significance of the between-gender asymmetry score differences. C_p, L_p, γ, λ, E_{loc} and E_{glob} denote the clustering coefficient, characteristic path length, normalized clustering coefficient, normalized shortest path length, local efficiency and global efficiency, respectively. Positive t-scores of Females and Males indicate rightward asymmetries and vice versa. Positive t-scores of Females–Males indicate females' more significant rightward asymmetries and vice versa. Significant effects ($P<0.05$) are indicated by bold text.

Results

Global properties of the hemispheric networks

Small-worldness and efficiency

In this study we constructed functional networks based on separate hemispheres rather than on the whole brain. We found that over the sparsity range of 10%~46%, the γ were larger than 1 (i.e., the C_p for these networks were larger than those of their matched random networks) and the λ were nearly 1 (i.e., the L_p for these networks were comparable to those of their matched random networks) for four subgroups (2 hemispheres × 2 genders) of functional networks (Fig. 1). When evaluating the global network parameters using a summary parameter $\sigma = \gamma / \lambda$, we observed that σ were larger than 1.2 over the sparsity range of 10%~46% in four subgroups of functional networks (Fig. S1 in the supplementary materials). These data underlie the reason why this range was used in the present study. Thus, these hemispheric networks exhibited prominent small-world properties, which was consistent with previous whole-brain functional network studies (Watts and Strogatz, 1998; Humphries et al., 2006). From the efficiency perspective, the global efficiencies of these networks were comparable to the matched random networks (Fig. 2A), but the local efficiencies of these networks were larger than the matched random networks (Fig. 2B). These results further support the small-worldness of these hemispheric networks by indicating that these networks are approximately efficient in global information processing but more efficient in local information processing compared with their matched random networks.

Hemispheric and gender effects

Neither the gender effect nor the hemispheric effect was significant on any of the six global network parameters ($P<0.05$). However, we observed a significant gender–hemisphere interaction on γ ($F=4.43$, $P=0.04$) (Table 2). Further t-test analysis indicated that this interaction resulted from a rightward asymmetry in males ($t=1.48$, $P=0.15$) but a leftward asymmetry in females ($t=-1.59$, $P=0.12$). Fig. 3 illustrates the global network parameters of the hemispheric networks of males and females.

The asymmetry score

None of the asymmetry scores of any of the six parameters was found to be significant ($P<0.05$) in either gender (Table 3). However, males tended to be more locally efficient in their right hemispheres (positive asymmetry scores of C_p, γ and E_{loc}) and females tended to be more locally efficient in their left hemispheres (negative asymmetry scores of C_p, γ and E_{loc}). When comparing the asymmetry scores of the six global parameters between males and females, we observed a significant gender-related difference only in γ ($t=-2.14$, $P<0.04$, female<male) (Table 3). This result was compatible with the gender–hemisphere interaction on γ shown above (Table 2). Of note, both males and females tended to be more globally efficient in their right hemispheres (positive asymmetry scores of E_{glob} and negative asymmetry scores of L_p and λ) (Table 3). However, there were no significant differences in the asymmetry scores of the three network parameters between males and females ($P>0.1$) (Table 3), which was consistent with the above results of non-significant gender effects by a two-way ANOVA (Table 2).

Table 4
The hubs of the hemispheric networks in both males and females.

Region	Classification	Normalized nodal parameters			Region	Classification	Normalized nodal parameters		
		Degree	Regional efficiency	BC			Degree	Regional efficiency	BC
Males: Left Hemisphere					***Females: Left Hemisphere***				
MCG	Paralimbic	1.43	1.14	2.57	**MTG**	Association	1.40	1.14	1.77
MTG	Association	1.39	1.14	2.11	**ITG**	Association	1.37	1.12	1.78
SFGdor	Association	1.39	1.14	1.95	**SFG**	Association	1.36	1.13	1.68
PreCG	Primary	1.37	1.13	1.83	FFG	Association	1.30	1.11	1.66
ITG	Association	1.36	1.13	1.99	MOG	Association	1.28	1.10	1.65
MOG	Association	1.32	1.11	1.64	PreCG	Primary	1.27	1.10	1.92
FFG	Association	1.29	1.10	1.70	**TPOsup**	Paralimbic	1.22	–	–
LING	Association	1.27	1.09	–	LING	Association	1.22	–	–
MFG	Association	1.25	1.09	–	**MCG**	Paralimbic	1.21	–	1.95
TPOsup	Paralimbic	–	–	1.68					
Males: Right Hemisphere					***Females: Right Hemisphere***				
MCG	Paralimbic	1.53	1.18	2.96	**ITG**	Association	1.48	1.16	2.61
ITG	Association	1.49	1.16	2.51	**MCG**	Paralimbic	1.44	1.15	2.61
MTG	Association	1.40	1.15	2.20	**TPOsup**	Paralimbic	1.43	1.14	2.09
STG	Association	1.37	1.13	1.62	**MTG**	Association	1.38	1.14	2.12
TPOsup	Paralimbic	1.37	1.13	2.08	STG	Association	1.36	1.12	1.67
SFG	Association	1.35	1.13	1.85	**SFG**	Association	1.31	1.11	1.75
MFG	Association	1.27	1.10	1.64	LING	Association	1.26	1.09	–
					FFG	Association	1.23	–	–
					MFG	Association	–	–	1.59

BC, betweenness centrality. "–" indicates that the value of the nodal parameter $X_i[X$ is the nodal degree (D_{nod}), nodal efficiency (E_{nod}) or nodal betweenness centrality (N_{bc})] in the regions was less than *mean* + *SD*. Hub regions identified in all four subgroups of networks are indicated by bold and shaded text. The abbreviation of each region can be found in Table 1.

Regional nodal properties of the hemispheric networks

Network hubs

In this study we identified hubs according to their regional nodal parameters, D_{nod}, E_{nod} and N_{bc}. Although a region could be identified as a hub according to a single regional nodal parameter, most hubs identified in this study were brain regions "in common" to all the three parameters. As shown in Table 4, five brain regions (the middle cingulate gyrus [MCG], the middle temporal gyrus [MTG], the dorsal superior frontal gyrus [SFGdor], the inferior temporal gyrus [ITG], the superior temporal pole [TPOsup]) were common hubs for the four subgroups of networks (for surface visualization, see Fig. 4). The lingual gyrus (LIN) and the fusiform gyrus (FFG) were hubs for all but the right hemispheric networks of males, and the middle frontal gyrus (MFG) was not a hub for the left hemispheric networks of females (Table 4, Fig. 4). The middle occipital gyrus (MOG) and the precentral gyrus (PreCG) were hubs only for the left hemispheric networks and the superior temporal gyrus (STG) was a hub only for the right hemispheric networks (Table 4, Fig. 4). Eight of the eleven hub regions were association cortices suggesting their critical roles in information transferring. Most of these hubs for hemispheric networks identified in the present study have formerly been observed to have a relatively shorter characteristic path length (Achard et al., 2006) or a higher betweenness centrality (He et al., 2009b) in networks based on the analysis of the whole brain.

Hemisphere-related differences

Two-way repeated-measures ANOVA revealed no significant gender effect or hemisphere–gender interaction but significant hemispheric effects on the regional nodal parameters of fifteen nodes ($P<0.05$, Bonferroni corrected) (Table 5, Fig. 5). Moreover, significant hemispheric effects on the three regional nodal parameters were observed on nearly the same nodes, except that the number of nodes whose betweenness centralities exhibited significant hemisphere-related differences was smaller. We found that seven brain regions exhibited significant left-greater-than-right

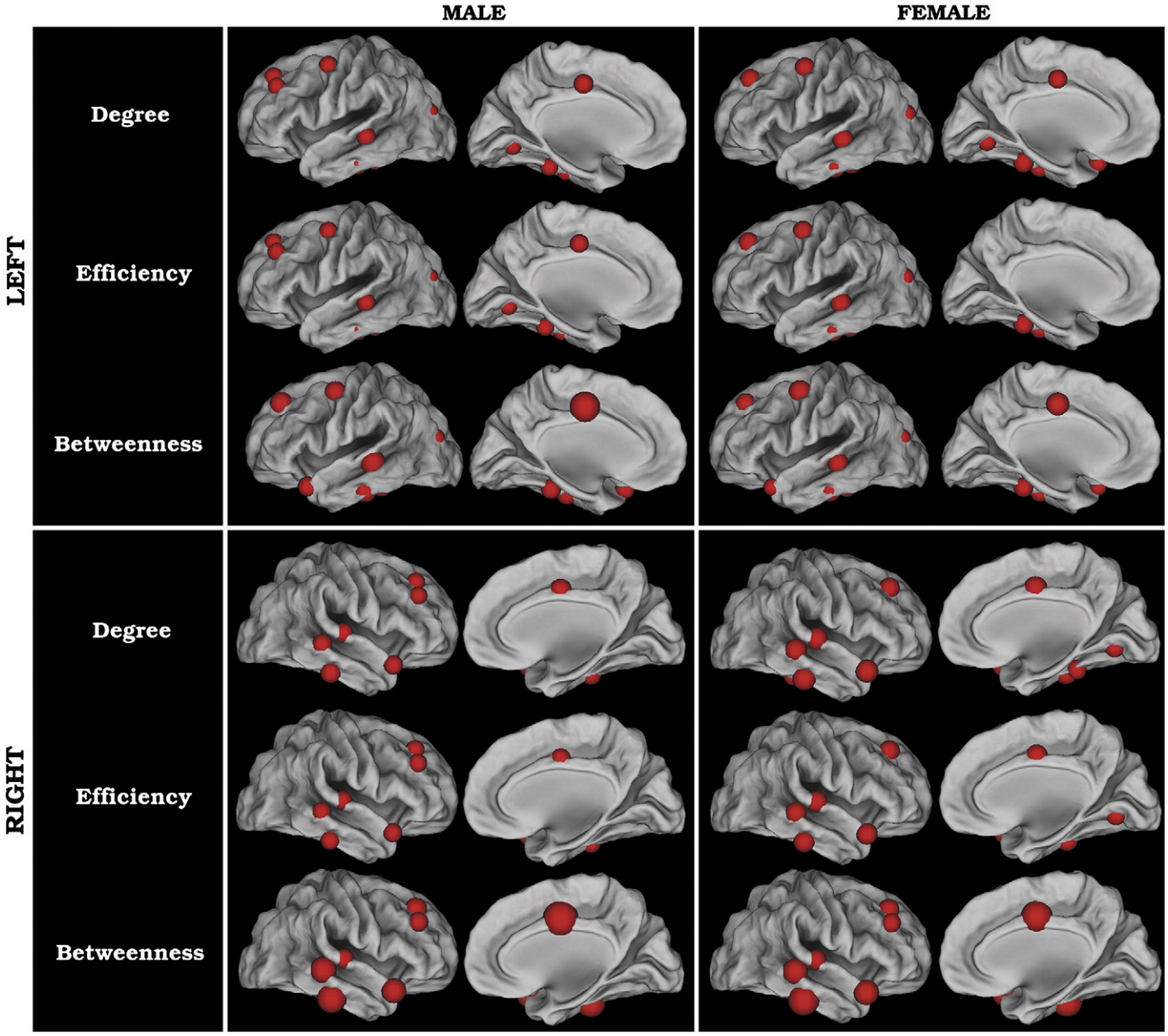

Fig. 4. The hubs in the hemispheric functional networks. The node sizes indicate their relative nodal degree (D_{nod}), nodal efficiency (E_{nod}) and nodal betweenness centrality (N_{bc}) within the subgroup of networks. Regions with any normalized nodal parameter $\bar{X}_i$ (X is D_{nod},E_{nod}, or N_{bc}) greater than $mean\left(\bar{X}_i\right) + SD\left(\bar{X}_i\right)$ were identified as hubs. Also see Table 4 for more details.

Table 5
Significant hemisphere effects on nodal characteristics revealed by two-way repeated-measures ANOVA.

Region	Classification	F-value (P-value)			Hub
		Degree	Regional efficiency	BC	
Left>right					
MOG	Association	98.64 (7.77×10^{-16})	80.93 (6.04×10^{-14})	66.73 (2.78×10^{-12})	Y
PreCG	Primary	50.36 (3.76×10^{-10})	55.92 (6.66×10^{-11})	79.45 (8.86×10^{-14})	Y
PCG	Paralimbic	42.52 (4.94×10^{-9})	29.05 (6.35×10^{-7})	11.65 (9.91×10^{-4})	N
REC	Paralimbic	26.06 (2.03×10^{-6})	23.70 (5.23×10^{-6})	–	N
SFGmed	Association	20.88 (1.66×10^{-5})	13.39 (4.40×10^{-4})	–	N
CAL	Primary	20.28 (2.14×10^{-5})	22.00 (1.05×10^{-5})	15.03 (2.10×10^{-4})	N
IOG	Association	9.58 [a] (0.0027)	12.82 (5.74×10^{-4})	–	N
Right>left					
STG	Association	40.41 (1.02×10^{-8})	40.04 (1.12×10^{-8})	16.28 (1.20×10^{-4})	Y
MCG	Paralimbic	36.19 (4.50×10^{-8})	42.37 (5.21×10^{-9})	22.10 (1.00×10^{-5})	Y
INS	Paralimbic	32.64 (1.64×10^{-7})	36.96 (3.42×10^{-8})	–	N
SMG	Association	21.22 (1.45×10^{-5})	25.82 (2.23×10^{-6})	–	N
IFGoperc	Association	19.81 (2.61×10^{-5})	11.73 (9.55×10^{-4})	–	N
TPOsup	Paralimbic	17.94 (5.80×10^{-5})	19.80 (2.62×10^{-5})	13.13 (4.96×10^{-4})	Y
ITG	Association	13.26 (4.69×10^{-4})	13.00 (5.28×10^{-4})	19.06 (3.59×10^{-5})	Y
SMA	Association	8.71[a] (0.0041)	12.47 (6.74×10^{-4})	—	N

BC, betweenness centrality. "–" indicates that the hemisphere effect was not significant. The threshold was $P<0.05$ (Bonferroni corrected).
[a] $P<0.005$ (uncorrected). The directions of hemispheric effects were determined by post hoc t-tests. "Y" indicates that the region has been identified as a "hub" of any of the four subgroups of networks and "N" indicates that the region is not a hub. The abbreviation of each region can be found in Table 1.

asymmetries mainly involving the frontal lobe regions (the medial superior frontal gyrus [SFGmed], the PreCG and the rectus gyrus [REC]) and the occipital lobe regions (the MOG, the calcarine cortex [CAL] and the inferior occipital gyrus [IOG]). Regions with significant right-greater-than-left asymmetries were predominantly located at the temporal lobe (the STG, the TPOsup, the superior marginal gyrus [SMG], the insula [INS] and the ITG).

The asymmetry score

Six nodes (the MOG, the PreCG, the PCG, the INS, the SMG and the STG) in the hemispheric networks of males and twelve nodes (the MOG, the PCG, the SFGmed, the REC, the middle orbital frontal cortex [ORBmid], the PreCG, the MCG, the STG, the SMA, the INS, the TPOsup and the cuneus [CUN]) in the networks of females were significantly asymmetric ($P<0.05$, Bonferroni corrected) (Table 6, Fig. 6). All six nodes in the networks of males and ten (except the CUN and the ORBmid) of twelve nodes in the networks of females have been observed to be asymmetric in the previous ANOVA analysis, and the asymmetries were in the same direction (Tables 5, 6). No node was significantly different between genders in the asymmetry score of any of its three nodal parameters ($P<0.05$, Bonferroni corrected). This result was compatible with the non-significant hemisphere–gender interaction on the regional nodal parameters shown above.

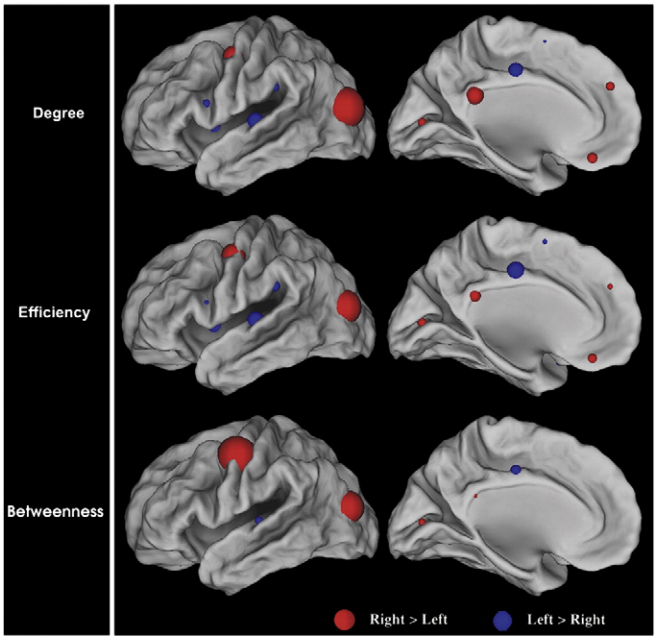

Fig. 5. Regions exhibited significant hemisphere-related differences in the regional nodal parameters. The node sizes indicate the relative significance of hemisphere-related differences in the nodal degree, nodal efficiency and nodal betweenness centrality. The red color represents rightward asymmetries, and the blue color represents leftward asymmetries. The threshold was $P<0.05$ (Bonferroni corrected). Also see Table 5 for more details.

Discussion

In this study we utilized R-fMRI and graph theoretical approaches to investigate the hemisphere- and gender-related differences in brain functional networks. The main findings are as follows: 1) the hemispheric networks exhibited small-world attributes (high clustering and short paths); 2) males tended to be more locally efficient in their right hemispheric networks, but females tended to be more locally efficient in their left hemispheric networks; 3) significant hemisphere-related differences in regional nodal parameters were observed in the fronto-occipital regions (rightward asymmetry) and temporal regions (leftward asymmetry).

Small-worldness of hemispheric functional networks of human brain

The small-world network introduced by Watts and Strogatz (1998) has made a tremendous impact on the study of numerous complex networks (Strogatz, 2001). The model characterizes the architecture of networks with well-connected local neighborhoods and a short mean distance between nodes. Recent studies have suggested that the human brain functional networks constructed from fMRI (Eguiluz et al., 2005; Salvador et al., 2005; Achard et al., 2006), EEG (Micheloyannis et al., 2006; Stam et al., 2007) and MEG (Stam, 2004) data have small-world properties. In this study we constructed functional networks based on separate hemispheres and also observed small-worldness (Figs. 1, 2, S1 (in the supplementary materials)). This finding indicates that the small-world topology is also a fundamental principle of the organization of hemispheric functional networks.

The small-world topology has a high clustering coefficient and short path length, indicating the local clustering, or cliquishness, of the connectivity network and the small geodesic distance between any pair of regions. Previous computational simulation studies have demonstrated that small-world topologies emerge when networks are evolved for high complexity (Sporns et al., 2000). Therefore small-

Table 6
Significant asymmetry scores of regional nodal parameters in males and females.

Region	Classification	T-Score (P-value)			Hub
		Degree	Regional efficiency	BC	
Males: left>right					
MOG	Association	−8.08 (1.08×10^{-9})	−7.90 (1.86×10^{-9})	−7.49 (6.42×10^{-9})	Y
PreCG	Primary	−7.67 (3.71×10^{-9})	−7.88 (1.95×10^{-9})	−9.71 (1.02×10^{-11})	Y
PCG	Paralimbic	−3.67 (7.52×10^{-4})	–	–	N
Males: right>left					
INS	Paralimbic	4.42 (8.26×10^{-5})	4.79 (2.73×10^{-5})	–	N
SMG	Association	3.88 (4.16×10^{-4})	4.22 (1.53×10^{-4})	3.69 (7.22×10^{-4})	N
STG	Association	3.75 (6.12×10^{-4})	3.74 (6.28×10^{-4})	–	Y
Females: left>right					
MOG	Association	−5.56 (1.22×10^{-6})	−5.24 (3.69×10^{-6})	−6.26 (1.08×10^{-7})	Y
PCG	Paralimbic	−4.27 (9.32×10^{-5})	−3.84 (3.67×10^{-4})	−3.46[a] (0.0012)	N
SFGmed	Association	−3.89 (3.14×10^{-4})	−3.36[a] (0.0015)	–	N
REC	Paralimbic	−3.62 (7.28×10^{-4})	−3.66 (6.45×10^{-4})	–	N
ORBmid	Paralimbic	−3.54 (9.27×10^{-4})	−3.13[a] (0.0030)	–	N
PreCG	Primary	−3.19[a] (0.0025)	−3.50 (0.0010)	−6.39 (6.79×10^{-8})	Y
Females: right>left					
MCG	Paralimbic	6.03 (2.45×10^{-7})	6.50 (4.70×10^{-8})	5.06 (6.92×10^{-6})	Y
STG	Association	5.55 (1.30×10^{-6})	5.07 (6.60×10^{-6})	–	Y
SMA	Association	3.79 (4.26×10^{-4})	4.30 (8.67×10^{-5})	–	N
INS	Paralimbic	3.67 (6.27×10^{-4})	4.02 (2.07×10^{-4})	–	N
CUN	Association	3.96 (2.51×10^{-4})	3.58 (8.18×10^{-4})	3.77 (4.53×10^{-4})	N
TPOsup	Paralimbic	3.21[a] (0.0024)	3.58 (8.21×10^{-4})	3.78 (4.41×10^{-4})	Y

BC, betweenness centrality. "–" indicates that the asymmetry score was not significant. The threshold was $P<0.05$ (Bonferroni corrected).

[a] $P<0.005$ (uncorrected). "Y" indicates that the region has been identified as a "hub" of any of the four subgroups of networks and "N" indicates that the region is not a hub. The abbreviation of each region can be found in Table 1.

world architecture of our hemispheric functional network represents an optimal organizational pattern according to evolution and development. In terms of information flow, high clustering allows modularized information processing, which is functionally segregated from one area to another, and short paths allow effective interactions or rapid transfer of information between regions, which is essential for functional integration. The coexistence of functional segregation and functional integration ensures the effective integration of multiple segregated sources of information in the brain (Tononi et al., 1994; Sporns et al., 2004; Sporns and Zwi, 2004). The small-worldness of hemispheric functional networks observed in this study indicates that information processing in separate hemispheres could be of similar efficiency as that in the whole brain.

Network local efficiency: right-lateralized in males but left-lateralized in females

In this study males tended to be more locally efficient in their right hemispheric networks and females tended to be more locally efficient in their left hemispheric networks (Tables 2, 3, Fig. 3). Sex differences in language and visuospatial performances have been well-documented with males performing better on visuospatial tasks, especially those involving mental rotation and spatial perception, and females performing better on language tasks, including phonological processing and verbal memory (Voyer et al., 1995; Kansaku and Kitazawa, 2001; Sommer et al., 2004). Functional neuroimaging studies demonstrated that in both genders language processing is generally more left-lateralized and visuospatial processing is generally more right lateralized (Maccoby and Jacklin, 1974; Halpern, 2000; Eagley et al., 2004). In combination with former findings, we speculate that the local efficiency of hemispheric networks might be associated with behavioral and cognitive differences between males and females. In the future, it would be interesting to explore the relationship between the network local efficiencies and behavioral and cognitive variables in genders such as the performances of language and visuospatial processing.

Network global efficiency: no significant hemisphere- or gender-related difference

As indicated by positive asymmetry scores of E_{glob} and negative asymmetry scores of L_p and λ (Table 3), both males and females tended to be more globally efficient in their right hemispheres. Nonetheless, we observed no hemisphere- or gender-related differences in the global efficiency of hemispheric functional networks (Tables 2, 3, Fig. 3). This indicates that the two hemispheres/genders are not significantly different in transferring information between brain regions. However, in a study by Gong et al. (2009b), the cortical networks of females were more efficient both locally and globally. In a study by Iturria-Medina et al. (in press), the right hemispheric networks were more efficient and interconnected than the left hemispheric networks. In a study by Yan et al. (2010), females had greater local efficiencies than males. The apparent discrepancies between the present results and those in the two former studies could stem from the following two aspects. Firstly, Gong et al. (2009b), Iturria-Medina et al. (in press) and Yan et al. (2010) all constructed networks based on structural connectivities, but the networks in the present study were based on functional connectivities. Although functional connectivities are closely related to structural connectivities, there are still some functional connectivities that cannot be explained by structural connectivities (Honey et al., 2009). Therefore, the hemisphere- and gender-related differences in structural organizations would not necessarily accompany differences in functional organizations. Secondly, we investigated the hemisphere- and gender-related differences based on the integrated global network parameters, and this integration may screen out some hemisphere- or gender-related differences at certain sparsities as have been observed in three former studies (Gong et al., 2009b; Iturria-Medina et al., in press; Yan et al., 2010).

Hemisphere-related differences in regional nodal parameters

Previous studies reported regional asymmetries based mainly on morphologic features or activation patterns of separate brain regions. In this study, the functional asymmetry of certain brain region was evaluated based on the relative importance of the region within the hemispheric network. Significant ($P<0.05$, Bonferroni corrected) leftward functional asymmetries were observed in the frontal (the SFGmed, the PreCG and the REC) and occipital (the MOG, the CAL and the IOG) regions, and significant rightward asymmetries were observed in the temporal regions (the STG, the TPOsup, the SMG, the INS and the ITG) (Tables 5, 6, Figs. 5, 6).

Leftward asymmetries

Significant leftward asymmetries were observed in three frontal regions (the SFGmed, the PreCG and the REC) in the present study

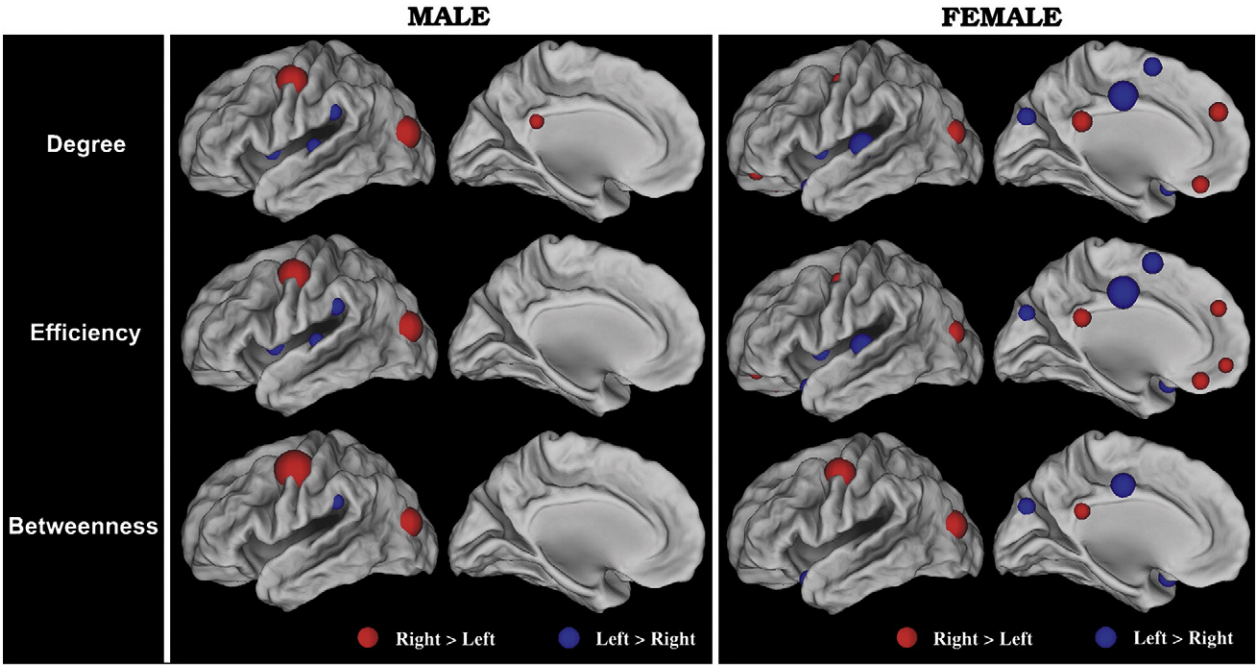

Fig. 6. Regions with significant asymmetry scores in males and females. The node sizes indicate the relative significance of asymmetry scores of the nodal degree, nodal efficiency and nodal betweenness centrality. The red color represents rightward asymmetries, and the blue color represents leftward asymmetries. The threshold was $P<0.05$ (Bonferroni corrected). Also see Table 6 for more details.

(Table 5, Fig. 5). The SFGmed, together with the PCG which was also observed to be leftward asymmetric in the present study, are two critical components of the so-called default mode network. These two regions have been observed to be structurally asymmetric in former studies (Paus et al., 1996; Luders et al., 2006). Moreover, Iturria-Medina et al. (in press) observed significant leftward structural asymmetry of these two regions using the betweenness centrality. Based on R-fMRI, Liu et al. (2009) found significant leftward asymmetries "along the cortical midline" in human brain. These results are consistent with the present study. The leftward asymmetry of the PreCG in right-handed subjects has been observed using various techniques (Melsbach et al., 1996; Amunts et al., 2000; Davatzikos and Bryan, 2002; Luders et al., 2006). The present finding of a significant leftward asymmetry of the PreCG in right-handed subjects is consistent with former findings. Another critical component of the motor system, the SMA, also exhibited significant functional asymmetry, but the asymmetry was of a rightward direction (Table 5).

As to the occipital regions, a consistent leftward structural asymmetry has been reported in post-mortem (Cunningham, 1892; Elliot-Smith, 1907) and *in vivo* structural imaging studies (Watkins et al., 2001; Toga and Thompson, 2003). Within the structural network based on diffusion tensor imaging (DTI), the MOG exhibited the most significant leftward asymmetry as assessed by the nodal betweenness centrality (Gong et al., 2009a). Therefore, the present leftward asymmetries of these occipital cortices are consistent with these findings based on structural images. However, Liu et al. (2009) observed a significant rightward asymmetry of the visual cortices based on R-fMRI. Using the betweenness centrality, Iturria-Medina et al. (in press) reported significant rightward asymmetries in the occipital regions. Liu et al. (2009) and Iturria-Medina et al. (in press) both attributed these rightward asymmetries to right-lateralized visuospatial processing. Further studies are expected to reconcile the apparent inconsistencies between the directions of asymmetries reported in the occipital regions.

Rightward asymmetries

In this study five temporal regions, the STG, the TPOsup, the SMG, the INS and the ITG, exhibited significant rightward asymmetries (Table 5). In several former studies (Watkins et al., 2001; Liu et al., 2009), the INS exhibited significant rightward structural or functional asymmetries and has been suggested to be very involved in the right-lateralized attentional system, which is important for detecting unattended events. Thus the present finding of a significant rightward asymmetry of the INS is consistent with these former findings. Other temporal regions that exhibited significant asymmetries in the present study, especially the STG, have been repeatedly reported to be asymmetric (Toga and Thompson, 2003), but the exact direction of these asymmetries has been quite inconsistent. Specifically, although numerous studies reported significant leftward asymmetries in these regions (Toga and Thompson, 2003), rightward asymmetries have also been demonstrated (Watkins et al., 2001; Luders et al., 2006). The inconsistencies among the exact direction of the asymmetries of these temporal regions needs to be further investigated.

Further considerations

Despite the present findings, this study on organizational pattern asymmetries in the human brain is still preliminary, and further studies on the following issues are expected. First, we observed significant hemisphere- and gender-related differences in the topological organizations of brain functional networks. However, some aspects of these differences observed in the present study are quite different from those based on structural networks (Gong et al., 2009b; Iturria-Medina et al., in press). As brain functional connectivities are closely related to the underlying structural connectivities (Honey et al., 2009), a further study simultaneously evaluating the topologies of functional and structural networks is expected. Second, we observed significant asymmetries in the topological organization of brain functional networks. As has been mentioned, brain asymmetries are closely related to lateralized behaviors. Thus further analysis of brain organizational asymmetries should be carried out for a better understanding of the basis of lateralized functions such as language and visuospatial processing. Third, changes of brain asymmetries are closely related to the pathophysiology of various brain diseases such as stroke and schizophrenia. For example, interhemispheric position asymmetries of homologous areas are repeatedly reported in stroke

subjects and these asymmetries are correlated with later clinical recovery (Liepert et al., 2000; Tecchio et al., 2006a, 2006b, 2007). Therefore, evaluating the topological organization of brain functional networks within hemispheres is likely to improve our knowledge about stroke and its clinical recovery. Similarly, the pathology of schizophrenia, which is closely related to disturbances of brain asymmetries (Bilder et al., 1999; Niznikiewicz et al., 2000; Sommer et al., 2001; Narr et al., 2001; Bleich-Cohen et al., 2009), could also be investigated from the perspective of brain network asymmetry.

Conclusion

To summarize, we evaluated the hemisphere- and gender-related differences in human brain functional networks based on R-fMRI. We observed that males and females have quite different asymmetric patterns in their network local efficiencies and suggest that these differences are closely related to the behavioral differences. Most regions that exhibited significant hemisphere-related differences in the present study have formerly been observed to be structurally or functionally asymmetric. Overall our results indicate that a complex brain network analysis could be a profitable tool for investigating individual differences in brain function. Further work could be conducted to examine whether these network properties are altered during normal development and aging, as well as under specific brain disorders.

Supplementary materials related to this article can be found online at doi:10.1016/j.neuroimage.2010.07.066.

Acknowledgments

The authors thank Dr. Yufeng Zang for kindly providing the dataset. This work was supported by the National Natural Science Foundation of China (grant nos. 30870667 and 30800249), Beijing Natural Science Foundation (grant no. 7102090), and the Scientific Research Foundation for the Returned Overseas Chinese Scholars (State Education Ministry, YH).

References

Achard, S., Bullmore, E., 2007. Efficiency and cost of economical brain functional networks. PLoS Comput. Biol. 3, e17.
Achard, S., Salvador, R., Whitcher, B., Suckling, J., Bullmore, E., 2006. A resilient, low-frequency, small-world human brain functional network with highly connected association cortical hubs. J. Neurosci. 26, 63–72.
Amunts, K., Jancke, L., Mohlberg, H., Steinmetz, H., Zilles, K., 2000. Interhemispheric asymmetry of the human motor cortex related to handedness and gender. Neuropsychologia 38, 304–312.
Bassett, D.S., Bullmore, E.T., 2009. Human brain networks in health and disease. Curr. Opin. Neurol. 22 (4), 340–347.
Bassett, D.S., Bullmore, E., Verchinski, B.A., Mattay, V.S., Weinberger, D.R., Meyer-Lindenberg, A., 2008. Hierarchical organization of human cortical networks in health and schizophrenia. J. Neurosci. 28, 9239–9248.
Bergerbest, D., Gabrieli, J.D., Whitfield-Gabrieli, S., Kim, H., Stebbins, G.T., Bennett, D.A., Fleischman, D.A., 2009. Age-associated reduction of asymmetry in prefrontal function and preservation of conceptual repetition priming. Neuroimage 45, 237–246.
Bilder, R.M., Wu, H., Bogerts, B., Ashtari, M., Robinson, D., Woerner, M., Lieberman, J.A., Degreef, G., 1999. Cerebral volume asymmetries in schizophrenia and mood disorders: a quantitative magnetic resonance imaging study. Int. J. Psychophysiol. 34, 197–205.
Biswal, B.B., Mennes, M., Zuo, X.N., Gohel, S., Kelly, C., Smith, S.M., Beckmann, C.F., Adelstein, J.S., Buckner, R.L., Colcombe, S., Dogonowski, A.M., Ernst, M., Fair, D., Hampson, M., Hoptman, M.J., Hyde, J.S., Kiviniemi, V.J., Kotter, R., Li, S.J., Lin, C.P., Lowe, M.J., Mackay, C., Madden, D.J., Madsen, K.H., Margulies, D.S., Mayberg, H.S., McMahon, K., Monk, C.S., Mostofsky, S.H., Nagel, B.J., Pekar, J.J., Peltier, S.J., Petersen, S.E., Riedl, V., Rombouts, S.A., Rypma, B., Schlaggar, B.L., Schmidt, S., Seidler, R.D., Siegle, G.J., Sorg, C., Teng, G.J., Veijola, J., Villringer, A., Walter, M., Wang, L., Weng, X.C., Whitfield-Gabrieli, S., Williamson, P., Windischberger, C., Zang, Y.F., Zhang, H.Y., Castellanos, F.X., Milham, M.P., 2010. Toward discovery science of human brain function. Proc. Natl Acad. Sci. USA 107, 4734–4739.
Biswal, B., Yetkin, F.Z., Haughton, V.M., Hyde, J.S., 1995. Functional connectivity in the motor cortex of resting human brain using echo-planar MRI. Magn. Reson. Med. 34, 537–541.
Bleich-Cohen, M., Hendler, T., Kotler, M., Strous, R.D., 2009. Reduced language lateralization in first-episode schizophrenia: an fMRI index of functional asymmetry. Psychiatry Res. 171, 82–93.
Bullmore, E., Sporns, O., 2009. Complex brain networks: graph theoretical analysis of structural and functional systems. Nat. Rev. Neurosci. 10, 186–198.
Cunningham, D. (Ed.), 1892. Contribution to the Surface Anatomy of the Cerebral Hemispheres. Royal Irish Academy, Dublin.
Davatzikos, C., Bryan, R.N., 2002. Morphometric analysis of cortical sulci using parametric ribbons: a study of the central sulcus. J. Comput. Assist. Tomogr. 26, 298–307.
Eagley, A.H., Beall, A.E., Sternberg, R.J., 2004. The Psychology of Gender. The Guilford Press, New York.
Eguiluz, V.M., Chialvo, D.R., Cecchi, G.A., Baliki, M., Apkarian, A.V., 2005. Scale-free brain functional networks. Phys. Rev. Lett. 94, 018102.
Elliot-Smith, G., 1907. A new topographical survey of the human cerebral cortex, being an account of the distribution of the anatomically distinct cortical areas and their relationship to the cerebral sulci. J. Anat. Physiol. (London) 41, 237–254.
Fox, M.D., Raichle, M.E., 2007. Spontaneous fluctuations in brain activity observed with functional magnetic resonance imaging. Nat. Rev. Neurosci. 8, 700–711.
Freeman, L.C., 1977. Set of measures of centrality based on betweenness. Sociometry 40, 35–41.
Gong, G., He, Y., Concha, L., Lebel, C., Gross, D.W., Evans, A.C., Beaulieu, C., 2009a. Mapping anatomical connectivity patterns of human cerebral cortex using in vivo diffusion tensor imaging tractography. Cereb. Cortex 19, 524–536.
Gong, G., Rosa-Neto, P., Carbonell, F., Chen, Z.J., He, Y., Evans, A.C., 2009b. Age- and gender-related differences in the cortical anatomical network. J. Neurosci. 29, 15684–15693.
Good, C.D., Johnsrude, I., Ashburner, J., Henson, R.N., Friston, K.J., Frackowiak, R.S., 2001. Cerebral asymmetry and the effects of sex and handedness on brain structure: a voxel-based morphometric analysis of 465 normal adult human brains. Neuroimage 14, 685–700.
Hagmann, P., Kurant, M., Gigandet, X., Thiran, P., Wedeen, V.J., Meuli, R., Thiran, J.P., 2007. Mapping human whole-brain structural networks with diffusion MRI. PLoS ONE 2, e597.
Hagmann, P., Cammoun, L., Gigandet, X., Meuli, R., Honey, C.J., Wedeen, V.J., Sporns, O., 2008. Mapping the structural core of human cerebral cortex. PLoS Biol. 6, e159.
Halpern, D.F., 2000. Sex Differences in Cognitive Abilities, 3rd ed. Erlbaum, Mahwah, NJ.
Hamilton, C., 2008. Cognition and Sex Differences. Palgrave Macmillan, New York.
He, Y., Evans, A., 2010. Graph theoretical modeling of brain connectivity. Curr. Opin. Neurol. 23, 341–350.
He, Y., Chen, Z.J., Evans, A.C., 2007. Small-world anatomical networks in the human brain revealed by cortical thickness from MRI. Cereb. Cortex 17, 2407–2419.
He, Y., Chen, Z., Gong, G., Evans, A., 2009a. Neuronal networks in Alzheimer's disease. Neuroscientist 15, 333–350.
He, Y., Dagher, A., Chen, Z., Charil, A., Zijdenbos, A., Worsley, K., Evans, A., 2009b. Impaired small-world efficiency in structural cortical networks in multiple sclerosis associated with white matter lesion load. Brain 132, 3366–3379.
He, Y., Wang, J., Wang, L., Chen, Z.J., Yan, C., Yang, H., Tang, H., Zhu, C., Gong, Q., Zang, Y., Evans, A.C., 2009c. Uncovering intrinsic modular organization of spontaneous brain activity in humans. PLoS ONE 4, e5226.
Heim, S., Eulitz, C., Elbert, T., 2003. Altered hemispheric asymmetry of auditory N100m in adults with developmental dyslexia. NeuroReport 14, 501–504.
Hiscock, M., Inch, R., Jacek, C., Hiscock-Kalil, C., Kalil, K.M., 1994. Is there a sex difference in human laterality? I. An exhaustive survey of auditory laterality studies from six neuropsychology journals. J. Clin. Exp. Neuropsychol. 16, 423–435.
Hiscock, M., Israelian, M., Inch, R., Jacek, C., Hiscock-Kalil, C., 1995. Is there a sex difference in human laterality? II. An exhaustive survey of visual laterality studies from six neuropsychology journals. J. Clin. Exp. Neuropsychol. 17, 590–610.
Honey, C.J., Sporns, O., Cammoun, L., Gigandet, X., Thiran, J.P., Meuli, R., Hagmann, P., 2009. Predicting human resting-state functional connectivity from structural connectivity. Proc. Natl Acad. Sci. USA 106, 2035–2040.
Humphries, M.D., Gurney, K., Prescott, T.J., 2006. The brainstem reticular formation is a small-world, not scale-free, network. Proc. Biol. Sci. 273, 503–511.
Iturria-Medina, Y., Fernandez, A.P., Morris, D.M., Canales-Rodriguez, E.J., Haroon, H.A., Penton, L.G., Augath, M., Garcia, L.G., Logothetis, N., Parker, G.J., Melie-Garcia, L., in press. Brain Hemispheric Structural Efficiency and Interconnectivity Rightward Asymmetry in Human and Nonhuman Primates. Cereb Cortex. doi:10.1093/cercor/bhq058.
Kansaku, K., Kitazawa, S., 2001. Imaging studies on sex differences in the lateralization of language. Neurosci. Res. 41, 333–337.
Kimura, D., 1999. Sex and Cognition.: A Bradford Book, MIT Press. MIT Press, Cambridge, Mass: A Bradford Book.
Kovalev, V.A., Kruggel, F., von Cramon, D.Y., 2003. Gender and age effects in structural brain asymmetry as measured by MRI texture analysis. Neuroimage 19, 895–905.
Kulynych, J.J., Vladar, K., Jones, D.W., Weinberger, D.R., 1994. Gender differences in the normal lateralization of the supratemporal cortex: MRI surface-rendering morphometry of Heschl's gyrus and the planum temporale. Cereb. Cortex 4, 107–118.
Lancaster, J.L., Kochunov, P.V., Thompson, P.M., Toga, A.W., Fox, P.T., 2003. Asymmetry of the brain surface from deformation field analysis. Hum. Brain Mapp. 19, 79–89.
Latora, V., Marchiori, M., 2001. Efficient behavior of small-world networks. Phys. Rev. Lett. 87, 198701.
Leonard, C.M., Eckert, M.A., 2008. Asymmetry and dyslexia. Dev. Neuropsychol. 33, 663–681.
Leonard, C.M., Eckert, M.A., Lombardino, L.J., Oakland, T., Kranzler, J., Mohr, C.M., King, W.M., Freeman, A., 2001. Anatomical risk factors for phonological dyslexia. Cereb. Cortex 11, 148–157.

Liepert, J., Bauder, H., Wolfgang, H.R., Miltner, W.H., Taub, E., Weiller, C., 2000. Treatment-induced cortical reorganization after stroke in humans. Stroke 31, 1210–1216.
Liu, H., Stufflebeam, S.M., Sepulcre, J., Hedden, T., Buckner, R.L., 2009. Evidence that functional asymmetry of the human brain is controlled by multiple factors. Proc. Natl Acad. Sci USA 106, 20499–20503.
Luders, E., Narr, K.L., Thompson, P.M., Rex, D.E., Jancke, L., Toga, A.W., 2006. Hemispheric asymmetries in cortical thickness. Cereb. Cortex 16, 1232–1238.
Maccoby, E.E., Jacklin, C.N. (Eds.), 1974. The Psychology of Sex Differences. Stanford University Press, Standford, CA.
Maslov, S., Sneppen, K., 2002. Specificity and stability in topology of protein networks. Science 296, 910–913.
Melsbach, G., Wohlschlager, A., Spiess, M., Gunturkun, O., 1996. Morphological asymmetries of motoneurons innervating upper extremities: clues to the anatomical foundations of handedness? Int. J. Neurosci. 86, 217–224.
Micheloyannis, S., Pachou, E., Stam, C.J., Vourkas, M., Erimaki, S., Tsirka, V., 2006. Using graph theoretical analysis of multi channel EEG to evaluate the neural efficiency hypothesis. Neurosci. Lett. 402, 273–277.
Milo, R., Shen-Orr, S., Itzkovitz, S., Kashtan, N., Chklovskii, D., Alon, U., 2002. Network motifs: simple building blocks of complex networks. Science 298, 824–827.
Narr, K., Thompson, P., Sharma, T., Moussai, J., Zoumalan, C., Rayman, J., Toga, A., 2001. Three-dimensional mapping of gyral shape and cortical surface asymmetries in schizophrenia: gender effects. Am. J. Psychiatry 158, 244–255.
Narr, K.L., Bilder, R.M., Luders, E., Thompson, P.M., Woods, R.P., Robinson, D., Szeszko, P.R., Dimtcheva, T., Gurbani, M., Toga, A.W., 2007. Asymmetries of cortical shape: effects of handedness, sex and schizophrenia. Neuroimage 34, 939–948.
Newman, M.E.J., 2003. The structure and function of complex networks. SIAM Rev. 45, 167–256.
Niznikiewicz, M., Donnino, R., McCarley, R.W., Nestor, P.G., Iosifescu, D.V., O'Donnell, B., Levitt, J., Shenton, M.E., 2000. Abnormal angular gyrus asymmetry in schizophrenia. Am. J. Psychiatry 157, 428–437.
Paus, T., Otaky, N., Caramanos, Z., MacDonald, D., Zijdenbos, A., D'Avirro, D., Gutmans, D., Holmes, C., Tomaiuolo, F., Evans, A.C., 1996. In vivo morphometry of the intrasulcal gray matter in the human cingulate, paracingulate, and superior-rostral sulci: hemispheric asymmetries, gender differences and probability maps. J. Comp. Neurol. 376, 664–673.
Pujol, J., Lopez-Sala, A., Deus, J., Cardoner, N., Sebastian-Galles, N., Conesa, G., Capdevila, A., 2002. The lateral asymmetry of the human brain studied by volumetric magnetic resonance imaging. Neuroimage 17, 670–679.
Salvador, R., Suckling, J., Schwarzbauer, C., Bullmore, E., 2005. Undirected graphs of frequency-dependent functional connectivity in whole brain networks. Philos. Trans. R. Soc. Lond. B Biol. Sci. 360, 937–946.
Shaywitz, B.A., Shaywitz, S.E., Pugh, K.R., Constable, R.T., Skudlarski, P., Fulbright, R.K., Bronen, R.A., Fletcher, J.M., Shankweiler, D.P., Katz, L., et al., 1995. Sex differences in the functional organization of the brain for language. Nature 373, 607–609.
Sommer, I., Ramsey, N., Kahn, R., Aleman, A., Bouma, A., 2001. Handedness, language lateralisation and anatomical asymmetry in schizophrenia: meta-analysis. Br. J. Psychiatry 178, 344–351.
Sommer, I.E., Aleman, A., Bouma, A., Kahn, R.S., 2004. Do women really have more bilateral language representation than men? A meta-analysis of functional imaging studies. Brain 127, 1845–1852.
Sporns, O., Zwi, J.D., 2004. The small world of the cerebral cortex. Neuroinformatics 2, 145–162.
Sporns, O., Tononi, G., Edelman, G.M., 2000. Theoretical neuroanatomy: relating anatomical and functional connectivity in graphs and cortical connection matrices. Cereb. Cortex 10, 127–141.
Sporns, O., Chialvo, D.R., Kaiser, M., Hilgetag, C.C., 2004. Organization, development and function of complex brain networks. Trends Cogn. Sci. 8, 418–425.
Stam, C.J., 2004. Functional connectivity patterns of human magnetoencephalographic recordings: a 'small-world' network? Neurosci. Lett. 355, 25–28.
Stam, C.J., Jones, B.F., Nolte, G., Breakspear, M., Scheltens, P., 2007. Small-world networks and functional connectivity in Alzheimer's disease. Cereb. Cortex 17, 92–99.
Strogatz, S.H., 2001. Exploring complex networks. Nature 410, 268–276.
Tecchio, F., Zappasodi, F., Pasqualetti, P., Tombini, M., Caulo, M., Ercolani, M., Rossini, P.M., 2006a. Long-term effects of stroke on neuronal rest activity in rolandic cortical areas. J. Neurosci. Res. 83, 1077–1087.
Tecchio, F., Zappasodi, F., Tombini, M., Oliviero, A., Pasqualetti, P., Vernieri, F., Ercolani, M., Pizzella, V., Rossini, P.M., 2006b. Brain plasticity in recovery from stroke: an MEG assessment. Neuroimage 32, 1326–1334.
Tecchio, F., Zappasodi, F., Tombini, M., Caulo, M., Vernieri, F., Rossini, P.M., 2007. Interhemispheric asymmetry of primary hand representation and recovery after stroke: a MEG study. Neuroimage 36, 1057–1064.
Toga, A.W., Thompson, P.M., 2003. Mapping brain asymmetry. Nat. Rev. Neurosci. 4, 37–48.
Tononi, G., Sporns, O., Edelman, G.M., 1994. A measure for brain complexity: relating functional segregation and integration in the nervous system. Proc. Natl Acad. Sci. USA 91, 5033–5037.
Tzourio-Mazoyer, N., Landeau, B., Papathanassiou, D., Crivello, F., Etard, O., Delcroix, N., Mazoyer, B., Joliot, M., 2002. Automated anatomical labeling of activations in SPM using a macroscopic anatomical parcellation of the MNI MRI single-subject brain. Neuroimage 15, 273–289.
Voyer, D., Voyer, S., Bryden, M.P., 1995. Magnitude of sex differences in spatial abilities: a meta-analysis and consideration of critical variables. Psychol. Bull. 117, 250–270.
Wang, J., Zuo, X., He, Y., 2010. Graph-based network analysis of resting-state functional MRI. Front. Syst. Neurosci. 4, 16.
Watkins, K.E., Paus, T., Lerch, J.P., Zijdenbos, A., Collins, D.L., Neelin, P., Taylor, J., Worsley, K.J., Evans, A.C., 2001. Structural asymmetries in the human brain: a voxel-based statistical analysis of 142 MRI scans. Cereb. Cortex 11, 868–877.
Watts, D.J., Strogatz, S.H., 1998. Collective dynamics of 'small-world' networks. Nature 393, 440–442.
Yan, C.G., Zang, Y.F., 2010. DPARSF: a MATLAB toolbox for "pipeline" data analysis of resting-state fMRI. Front. Syst. Neurosci. 4, 13.
Yan, C.G., Gong, G.L., Wang, J.H., Wang, D.Y., Liu, D.Q., Chen, C.Z., Evans, Z.J., Zang, A., He, Y.F., Liu, D.Q., 2010. Sex- and brain size-related small-world structural cortical networks in young adults: a DTI tractography study. Cereb Cortex. doi:10.1093/cencor/bhq111.
Zhang, D., Raichle, M.E., 2010. Disease and the brain's dark energy. Nat. Rev. Neurol. 6, 15–28.